PHYSICAL REVIEW B VOLUME 17, NUMBER 8 15 APRIL 1978

Damping of electron-hole-droplet motion. I. Deformation potential scattering

D. S. Pan, D. L. Smith, and T. C. McGill
California Institute of Technology, Pasadena, California 91125
(Received 14 November 1977)

We report on a study of the damping of electron-hole-droplet (EHD) motion due to scattering by acoustical phonons coupled by the deformation-potential mechanism. Screening by the electrons and holes is taken into account in the random-phase approximation. Numerical results are presented for Ge in the low-velocity limit, EHD velocities less than the sound velocity, and high-velocity limit, velocities greater than the sound velocity. The low-velocity results are found to be in good agreement with the values of the phonon damping measured by an ultrasonic-absorption experiment. The results suggest that in recent measurements of EHD motion one must take into account driving forces produced by, perhaps, a phonon wind. In the high-velocity case the damping is found to be sufficiently large to make it unlikely that velocities greater than the sound velocity will be observed experimentally.

I. INTRODUCTION

The condensation of excitons into electron-hole droplets (EHD) in Ge and Si have been studied extensively.[1] Recently, there have been a number of experimental investigations[2-10] which give information on the interaction between acoustical phonons and EHD. These experiments may be divided into two classes.

The first class of experiments measures the damping of the drops by applying a known driving force.[2-7] The ultrasonic-absorption experiments have been interpreted in terms of drops being accelerated by the dynamic deformation from ultrasound and dissipating energy because of interaction with thermal lattice phonons. From the temperature dependence of the absorption of ultrasound at 160 MHz, the deduced momentum relaxation time is about 1 nsec at 2.4 °K.[2,3] Ultrasound in the gigahertz range couples with the capillary-wave oscillations of drops. In this case, the deduced momentum relaxation time is about 7 nsec at 1.8 °K.[4] Static nonuniform stress on the crystal also accelerates the drops. Experiments measuring the mobility of the EHD by setting up a static inhomogeneous deformation field give a relaxation time of roughly 6 nsec at 1.8 °K.[5] Droplets have also been shown to be driven by a wind of phonons,[6] and to be carried along by a current of free electrons and holes in an electric field.[7] However, for both the phonon wind and current drag, the forces were not accurately known.

The second class of experiments measures the arrival time of the EHD at some point in the crystal remote from the site of droplet generation.[8-10] The drops start with an initial drift velocity and their velocity decreases as a function of time or distance. Junction noise experiments[8] suggest that EHD can move a distance of about 0.3 mm. Assuming no external force, the observed motion indicates a momentum relaxation time of about 1 μsec.[8] Doppler-shifted light scattering experiments[9] have shown droplet motion in a direct fashion; the observed relaxation time is roughly 100 μsec (assuming no external force). In both experiments, the initial velocities of EHD are less than sound velocity. However, time and spatially resolved light-scattering experiments suggest that the initial droplet velocities can even exceed the sound velocity[10] in the crystal when the drops are formed by a short, high-intensity laser pulse; droplets are observed at a distance of about 5 mm from the excitation point and the damping is reported to be nonlinear.[10]

Theoretically, Keldysh[11,12] has pointed out that the motion of EHD in pure Ge should be damped by the interaction of the carriers in the EHD with acoustical phonons.

Using deformation-potential coupling, Keldysh calculated the damping rate (time derivative of the droplet drift velocity) in Ge as a function of temperature for droplet velocities much less than the sound velocity.[11,12] In this low-velocity regime, the damping rate is linear with velocity. The results of these calculations were in reasonable qualitative agreement with damping rates deduced from ultrasonic-absorption measurements[2,3] and from droplet motion in an inhomogeneous deformation field.[5] However, if the junction noise experiments and the light scattering experiments are interpreted in terms of droplet motion, either the phonon damping of the droplet motion must be much smaller than calculated by Keldysh or the droplets observed in these experiments were pushed along by some external force (e.g., a phonon wind). In other words, with the large damping rate computed by Keldysh, droplets could not move the distances observed in the junction noise and time and spatially resolved light scattering experiments unless they were pushed.

In deriving his results, Keldysh did not consider any modification of the free-carrier electron-phonon interaction for the carriers inside the EHD. However, one might expect that this interaction is screened by the carriers in the EHD. Such screening significantly reduces the "bare" electron-phonon interactions in a metal,[13] and one might expect a similar large reduction in the damping of EHD motion due to screening. Because EHD is a two-component system, the screening is more complicated than in a metal. The deformation of the lattice produced by an acoustical phonon is not an electrostatic perturbation and the polarizations of the electrons and holes in the EHD produced by this perturbation may have either the same or opposite phase.

The main purposes of this paper are twofold: first, to examine the effect that screening by the carriers in the EHD has on the damping of EHD motion; second, to investigate the damping of the droplet motion in Ge for velocities greater than the sound velocity.

We adopt the approach that the screening of the bare perturbation by the carriers in the EHD is calculated in the random-phase approximation (RPA). General results are derived for the low-velocity damping rate from the entropy production rate,[14] similar to those used in the theory of metal resistivity. This general result is evaluated by making use of some simplifying approximations to the details of conduction- and valence-band anisotropies. The result is equivalent to Keldysh's damping formula for a spherical band structure and a single effective deformation-potential constant.

In the high-velocity limit, the approximations to the distribution function used in the low-velocity limit are not valid. The distribution function for electrons and holes is assumed to be a shifted Fermi distribution function for zero temperature and the damping rate is calculated from a momentum balance equation.

We find that screening does not change qualitatively the damping of the EHD motion. The magnitude of the damping is changed by about a factor of 2 from a similar unscreened calculation. Our results are in semiquantitative agreement with the results of the ultrasonic attenuation experiments[2-4] and, hence, are in disagreement with the dynamical measurements[8,9] of EHD motion when interpreted without a driving force. Therefore, we conclude that droplets observed in junction noise and light scattering experiments are being pushed.

Our calculation of the damping rate in the high-velocity limit is some three orders magnitude larger than that obtained by interpreting the results of experiments in which EHD motion was observed following a strong pulse excitation.[10] Thus, droplets moving at velocities greater than the sound velocity would be very rapidly damped. We believe the very high initial velocities reported in Ref. 10 should not be interpreted in terms of droplet motion. Subsequent motion, at lower velocities, may be interpreted as due to a phonon wind pushing the droplets.

This paper is divided into five major sections as follows: In Sec. II, we consider the screening by the two components EHD on the bare electron-phonon interactions. Section III outlines the calculations of the damping coefficient for low-velocity droplet motion in cubic semiconductors. Section IV contains the calculation of the phonon damping coefficients of EHD in Ge in the low-velocity limit. Section V treats the phonon damping of droplet motion in Ge when the droplet velocity exceeds the velocity of sound. In Sec. VI, we give results, conclusion, and summarization.

II. SCREENING OF CARRIER-PHONON INTERACTION IN EHD

In most transport problems in semiconductors the low density of carriers means that we can neglect the screening of the carrier-phonon interaction.[14] However, in the EHD the density of carriers (2×10^{17} cm^{-3} in Ge) is sufficiently high that screening may play an important role. A simple estimate shows that the Thomas-Fermi screening wave vector q_{FT} is about 5×10^{6} cm^{-1} for the EHD in Ge. This value of q_{FT} is actually larger than the characteristic wave vector of the phonons which play a role in the scattering in the EHD; the Fermi wave vector for EHD is about 2×10^{6} cm^{-1} in Ge. Hence, we must consider the role of screening in the effective carrier-phonon interaction in EHD.

This problem is further complicated by the fact that EHD is a two-component quantum plasma. Therefore, we must consider the screening response from both carrier types each responding to the perturbation produced by their respective deformation-potential coupling. Since the deformation-potential coupling is not electrostatic, the electrons and holes may respond with different magnitudes and phases which are not simply given by signs of these charges. Thus, the screening response cannot be gauged by a single dielectric function.

In this section, we calculate the response of the electrons and holes to the carrier-phonon interaction. The responses are calculated in the random-phase approximation.

A. Derivation of screened interaction in RPA

The electrons and holes in the EHD are treated on the basis of the effective mass approximation.

The band structure is taken to be that in the elemental semiconductors Si and Ge and the III-V semiconductors with indirect gaps. The conduction band is assumed to have a number of equivalent valleys ν; the valence bands are assumed to consist of four degenerate bands at the zone center. The conduction-band valleys are assumed to be ellipsoidal with an energy for the nth valley given by $E_n^e(\vec{k})$. The four hole valence bands are assumed to have energies given by $E_n^h(\vec{k})$ where n labels the different valence bands. For this case, the single-particle Hamiltonian is given by

$$H_0 = 2\sum_{n=1}^{\nu}\sum_{\vec{k}} E_n^e(k) a_{\vec{k}n}^\dagger a_{\vec{k}n} + \sum_{n=1}^{4}\sum_{\vec{k}} E_n^h(\vec{k}) b_{\vec{k}n}^\dagger b_{\vec{k}n}, \quad (2.1)$$

where $a_{\vec{k}n}^\dagger$ creates an electron in the state with wave vector $\vec{k}$ in the nth valley and $b_{\vec{k}n}^\dagger$ creates a hole in the nth valence band in the state $\vec{k}$. The basis functions used in this second quantization are the Bloch functions from an appropriate band-structure calculation. The interaction between carriers can be written as

$$V_{cc} = \sum_{\vec{q}} \frac{2\pi e^2}{\kappa q^2} \rho(\vec{q})\rho(-\vec{q}), \quad (2.2)$$

where κ is the static dielectric constant of the solid.[15] In Eq. (2.2) $\rho(\vec{q})$ is the charge-density operator for the electrons and holes.

$$\rho(\vec{q}) = \sum_{\vec{k},nn'} O_{\vec{k}+\vec{q}n,\vec{k}n'} b_{\vec{k}+\vec{q}n}^\dagger b_{\vec{k}n'} - \sum P_{\vec{k}+\vec{q}n,\vec{k}n'} a_{k+qn}^\dagger a_{\vec{k}n'}, \quad (2.3)$$

where

$$O_{\vec{k}+\vec{q}n,\vec{k}n'} = \langle \psi_{\vec{k}+\vec{q}n}^h \,|\, e^{i\vec{q}\cdot\vec{r}} \,|\, \psi_{\vec{k}n'}^h \rangle \quad (2.4)$$

and

$$P_{\vec{k}+\vec{q}n,\vec{k}n'} = \langle \psi_{\vec{k}+\vec{q}n}^e \,|\, e^{i\vec{q}\cdot\vec{r}} \,|\, \psi_{\vec{k}n'}^e \rangle . \quad (2.5)$$

In Eq. (2.4) and Eq. (2.5) $\psi_{\vec{k},n}^e$ and $\psi_{\vec{k},n}^h$ are the appropriate Bloch functions for electrons and holes, respectively. In our treatment here we will neglect the large-$\vec{q}$ components which arise from intervalley scattering. For single-valley scattering, we can take

$$P_{\vec{k}+\vec{q}n,\vec{k}n'} \cong \delta_{nn'}, \quad (2.6)$$

neglecting terms of order $\vec{q}$. For the valence band, no such simplification is possible.

The interactions of electrons and holes with phonons are of the general form

$$V_{e\text{-ph}} = \sum_{\vec{k},\vec{q},n\lambda} D_n^e(\vec{k}+\vec{q},\vec{k},\lambda)\, a_{\vec{k}+\vec{q}n}^\dagger a_{\vec{k}n} (A_{\vec{q}\lambda} + A_{-\vec{q}\lambda}^\dagger) \quad (2.7)$$

and

$$V_{h\text{-ph}} = \sum_{\vec{k},\vec{q}nn'} D_{nn'}^h(\vec{k}+\vec{q},\vec{k},\lambda)\, b_{\vec{k}+\vec{q}n}^\dagger b_{\vec{k}n'} (A_{\vec{q}\lambda} + A_{-\vec{q}\lambda}^\dagger), \quad (2.8)$$

where $D_{nn'}^h(\vec{k}+q,\vec{k},\lambda)$, and $D_n^e(\vec{k}+\vec{q},\vec{k},\lambda)$ are the matrix elements of the interaction between phonons and a single carrier, and $A_{\vec{q}\lambda}^\dagger$ is the creation operator of a phonon with wave vector $\vec{q}$ and polarization λ. The intervalley phonon scattering is neglected in Eq. (2.7).

The total Hamiltonian is

$$H = H^0 + V_{cc} + V_{e\text{-ph}} + V_{h\text{-ph}}. \quad (2.9)$$

Using the well-known equation-of-motion techniques and RPA,[16] we obtain the following expression for the induced charge density due to linear response to the phonon perturbation

$$\rho(\vec{q}) = \sum_{\lambda} c_\lambda(\vec{q})(A_{\vec{q}\lambda} + A_{-\vec{q}\lambda}^\dagger), \quad (2.10)$$

where $c(q)$ is given by

$$c_\lambda(\vec{q}) = \frac{1}{\epsilon(\vec{q})}\left(\sum_{\vec{k}nn'} \frac{D_{nn'}^h(\vec{k}+\vec{q},\vec{q},\lambda) O_{\vec{k}+\vec{q},n,\vec{k},n'}}{E_n^h(\vec{k}+\vec{q}) - E_{n'}^h(\vec{k})} - \sum_{\vec{k}n} \frac{D_n^e(\vec{k}+\vec{q},\vec{k},\lambda)}{E_n^e(\vec{k}+\vec{q}) - E_n^e(\vec{k})} + \text{c.c.}\right) \quad (2.11)$$

and $\epsilon(\vec{q})$ is the dielectric function of the two components EHD in the RPA.

$$\epsilon(\vec{q}) = 1 + \frac{8\pi e^2}{\kappa q^2}\left(\sum_{\vec{k}n} \frac{1}{E_n^e(\vec{k}) - E_n^e(\vec{k}+\vec{q})} + \sum_{\vec{k}nn'} \frac{|O_{\vec{k}+\vec{q},n,\vec{k},n'}|^2}{E_{n'}^h(\vec{k}) - E_n^h(\vec{k}+\vec{q})}\right) \quad (2.12)$$

The summation in expressions for $c\lambda(\vec{q})$ and $\epsilon(\vec{q})$ are over the occupied single-particle states.

Adding the response given by Eqs. (2.10)–(2.12), we obtain expressions for the screened carrier-phonon interaction.

$$V_{e\text{-ph}}^S = \sum_{\vec{k}\vec{q}n\lambda} M_n^e(\vec{k}+\vec{q},\vec{k},\lambda) a_{\vec{k}+\vec{q}n}^\dagger a_{\vec{k}n} (A_{\vec{q}\lambda} + A_{-\vec{q}\lambda}^\dagger), \quad (2.13)$$

$$V_{h\text{-ph}}^S = \sum_{\vec{k}\vec{q}nn'\lambda} M_{nn'}^h(\vec{k}+\vec{q},\vec{k},\lambda) b_{\vec{k}+\vec{q}n}^\dagger b_{\vec{k}n'} (A_{\vec{q}\lambda} + A_{-\vec{q}\lambda}^\dagger), \quad (2.14)$$

where M^e and M^h are given by

$$M_n^e(\vec{k}+\vec{q},\vec{k},\lambda) = D_n^e(\vec{k}+\vec{q},\vec{k},\lambda) + \frac{4\pi e^2}{\kappa q^2} c_\lambda(\vec{q}), \quad (2.15)$$

$$M_{nn'}^h(\vec{k}+\vec{q},\vec{k},\lambda) = D_{nn'}^h(\vec{k}+\vec{q},\vec{k},\lambda) - \frac{4\pi e^2}{\kappa q^2} O_{\vec{k}+\vec{q},n,\vec{k}n'} c_\lambda(\vec{q}). \quad (2.16)$$

B. Symmetry considerations of response

Symmetry arguments may be used to simplify the potential due to the screening charge $V_p(\vec{q},\lambda)$ for certain directions of $\vec{q}$ and polarization λ. Writing $V_p(\vec{q},\lambda)$ in terms of the local strain induced by a given phonon mode $\epsilon_{ij}(\vec{q},\lambda)$ we have

$$V_p(\vec{q},\lambda)=\sum_{ij}F_{ij}(\vec{q})\epsilon_{ij}(\vec{q},\lambda)\,, \tag{2.17}$$

where $F_{ij}(\vec{q})$ is a second-rank tensor characterizing the linear response.

In the long-wavelength limit, which means that the phonon wave vector $\vec{q}$ is much smaller in magnitude than the Thomas-Fermi screening wave vector q_{FT}, the tensor $F_{ij}(\vec{q})$ is approximately independent of q and has the total cubic symmetry of the crystal. Thus, F_{ij} is a multiple of the unit tensor, and we have

$$V_p(\vec{q},\lambda)=F\sum_i\epsilon_{ii}(\vec{q},\lambda)\,. \tag{2.18}$$

The sum on the diagonal components is called the dilation $\Delta(\vec{q},\lambda)$. Hence, we have

$$V_p(\vec{q},\lambda)=F\Delta(\vec{q},\lambda)\,. \tag{2.19}$$

For any phonon mode or wave vector in the long-wavelength limit, only the dilational part of the local strain is screened.

However, in the range of the temperatures which are of interest around 2 °K, phonons with wavelengths of the order of the Fermi wave vector for the EHD make the primary contributions. These phonons have wavelengths which are on the order of the Thomas-Fermi wave vector. Thus, the long-wavelength limit is not valid in estimating the screening, and the above arguments must be modified to consider finite $\vec{q}$.

At finite $\vec{q}$, the symmetry arguments can be applied only along certain high-symmetry directions. For $\vec{q}$ along the [100], [110], and [111] directions, the phonons divide into totally transverse and longitudinal modes. In these directions in the diamond structure application of simple group-theoretical arguments[17] leads to the conclusion that there is no contribution to the potential in Eq. (2.17) from the transverse modes. Hence, for these high-symmetry directions there is no screening of the transverse modes. However, for arbitrary $\vec{q}$ the modes cannot be divided into transverse and longitudinal modes and all the modes are screened

III. DAMPING OF LOW-VELOCITY DROPLETS

Once the effective carrier's scattering matrix elements are known, the damping of the droplet motion can be calculated from transport theory. In the low-velocity limit, the damping should be linear. The well-known resistivity theory for a metal can be applied.[14] The calculations of the damping coefficient are outlined in this section.

The damping coefficient is defined by the equation

$$\frac{dv_i}{dt}=-\sum_j\gamma_{ij}v_j\,, \tag{3.1}$$

where v_i is the i^{th} component of the velocity of the droplet. In general γ_{ij} is a second-rank tensor. However, in cubic crystals of interest here γ_{ij} can be reduced to a scalar;

$$\gamma_{ij}=\gamma\delta_{ij}\,, \tag{3.2}$$

where δ_{ij} is the Kronecker delta.

To determine γ, we calculate the rate of entropy production.[14] The electrons in the EHD are characterized by a carrier distribution function $f_n(\vec{k})$ with n labeling the various conduction-band minimum. The deviation of each of these distribution functions as given by a function $\phi_n(k)$.

$$f_n(\vec{k})=f_n^0(\vec{k})-\phi_n(k)\frac{\partial f_n^0(\vec{k})}{\partial E_n^e(\vec{k})}\,, \tag{3.3}$$

where f_n^0 is the equilibrium distribution function. Similar equations hold for the holes. Throughout this discussion we consider for simplicity only the electron part of each expression.

The entropy production rate corresponding to the distribution function in Eq. (3.3) is given by[14]

$$\frac{dS}{dt}=\frac{1}{2k_BT^2}\int\int[\phi(\vec{k})-\phi(\vec{k}')]^2p(\vec{k}',\vec{k})\,d\vec{k}\,d\vec{k}'\,, \tag{3.4}$$

where k_B is the Boltzmann constant, T is the temperature of the EHD, and $p(\vec{k}',\vec{k})$ is the equilibrium transition probability for carriers from $\vec{k}$ to $\vec{k}'$. For lattice-phonon scattering, $p(\vec{k},\vec{k}')$ can be determined by calculating the scattering matrix for the effective carrier-phonon interaction in Eqs. (2.13) and (2.14), using Fermi's golden rule and averaging the matrix over the thermal equilibrium distribution function for carriers and phonons. The $\phi_n(\vec{k})$ is determined by a variational calculation in which the entropy production rate given in Eq. (3.3) is maximized. The total entropy production rate, $(dS/dt)_{\text{total}}$, is the sum of Eq. (3.3) over each conduction-band valley and each valence band.

The macroscopic rate of energy dissipation for a droplet of total mass M and velocity v is given by γMv^2. Equating the energy dissipation to the product of the temperature and the entropy production rate in Eq. (3.4), we obtain an expression for γ

$$\gamma=\frac{T}{Mv^2}\left(\frac{dS}{dt}\right)_{\text{total}}\,. \tag{3.5}$$

The macroscopic velocity $\vec{v}$ is given by

$$\vec{v} = -\int \vec{v}_n(\vec{k})\phi_n(\vec{k})\frac{\partial f_n^0(\vec{k})}{\partial E_n^e(\vec{k})}d^3k \Big/ \int f^0(\vec{k})\,d^3k\,, \qquad (3.6)$$

where $\vec{v}_n(\vec{k})$ is the group velocity for an electron in valley n with wave vector $\vec{k}$. The value of $\vec{v}$ is required to be independent of the valley and valence band over which the computation in Eq. (3.6) is evaluated. The inertial mass M is made up of a sum of terms of the form

$$\left| \int \hbar\vec{k}\phi_n(\vec{k})\frac{\partial f_n^0}{\partial E_n(\vec{k})}d^3k \right| \Big/ |\vec{v}|\,;$$

the sum runs over the conduction-band minimum with $\vec{k}$ measured from the conduction-band minimum and the various valence bands.

For our purpose here, we will simply take $\phi(k)$ of the form

$$\phi_n(\vec{k}) = \alpha_n \vec{k}\cdot\vec{u}\,, \qquad (3.7)$$

where $\vec{k}$ is measured from the conduction-band minimum, $\vec{u}$ is a unit vector in the direction of the velocity, and α_n is a parameter. The value of α_n for each valence band and conduction valley may be different. They are constrained to produce the same velocity of the drops. If the scattering function is very anisotropic, we might have to consider a more complicated trial function.[14,18,19]

Collecting the various results, we obtain finally

$$\gamma = \frac{1}{16\pi^5\hbar^2kT}\Bigg(2\sum_{n=1}^{\nu}\sum_{\lambda=1}^{3}\int (\alpha_n^e)^2\frac{(\hat{q}\cdot\hat{u})^2\omega(\vec{q},\lambda)\left|M_n^e(\vec{k}',\vec{k},\lambda)\right|^2}{(1-e^{-\hbar\omega(\vec{q},\lambda)/kT})(e^{\hbar\omega(\vec{q},\lambda)/kT}-1)}\frac{dG_n^e}{v_n^e(\vec{k})}\frac{dG_n^{e'}}{v_n^e(\vec{k}')}$$

$$+\sum_{n n'=1}^{4}\sum_{\lambda=1}^{3}\int \frac{[\hat{u}\cdot(\alpha_n^h\vec{k}_n^h-\alpha_{n'}^h\vec{k}_{n'}^h)]^2\omega(\vec{q},\lambda)\left|M_{n'n}^h(\vec{k}',\vec{k},\lambda)\right|^2}{(1-e^{-\hbar\omega(\vec{q},\lambda)/kT})(e^{\hbar\omega(\vec{q},\lambda)/kT}-1)}\frac{dG_n^h}{v_n^h(\vec{k})}\frac{dG_{n'}^h}{v_{n'}^h(\vec{k}')}\Bigg)$$

$$\times\left[\left(-2\sum_{n=1}^{\nu}\alpha_n^e\int\hbar\vec{k}_n^e(\vec{k}_n^e\cdot\hat{u})\frac{\partial f_n^0(\vec{k})}{\partial E_n^e(\vec{k})}\frac{d^3k_n^e}{(2\pi)^3}-\sum_n\alpha_n\int\hbar\vec{k}_n^h(\vec{k}_n^h\cdot\hat{u})\frac{\partial f_n^0(\vec{k})}{\partial E_n^h(\vec{k})}\frac{d^3k_n^h}{(2\pi)^3}\right)\cdot\vec{v}\right]^{-1}, \qquad (3.8)$$

with

$$\vec{q} = \vec{k}' - \vec{k}\,. \qquad (3.9)$$

Here $\omega(\vec{q},\lambda)$ is the angular frequency of a phonon with wave vector $\vec{q}$ and polarization λ, G_n is the surface area of the Fermi surface, and $\vec{v}_n(\vec{k})$ is the group velocity on the Fermi surface; $\vec{v}$ in the denominator of Eq. (3.8) is the velocity of droplet determined by Eq. (3.6) and (3.7) using $\alpha = 1$ for a conduction valley. The α_n^h's(α_n^e's) in Eq. (3.8) are constants for the n^{th} valence bands (conduction valley); they are determined from Eq. (3.6) and (3.7) by requiring that electrons and holes in EHD have the same velocity.

IV. PHONON DAMPING OF LOW-VELOCITY DROPLET MOTION IN Ge

The results for λ given in Eq. (3.8) may be evaluated using the measured deformation potentials,[19-24] phonon dispersion curves as computed from elastic constants,[19] the well-known band structure for Ge,[25] and the properties of the EHD.[26] This calculation would require extensive numerical work, particularly for the valence bands. For our purposes here, we want to examine the role of screening and to make simplifying approximations which will result in answers which should give a reasonable estimate of the magnitude of the damping.

A. Model for electrons

Herring and Vogt[19] have studied the expressions for the relaxation times appropriate to the mobility of electrons in Ge. They find their results are equivalent to a simplified model in which the anistropic scattering rates, variations in sound velocity, and contribution from all three phonons modes are replaced by a single phonon mode, the longitudinal mode, a single deformation-potential constant, and a spherically symmetric effective mass. The single deformation potential which is obtained by comparing their exact results with the simple model is[19]

$$\Xi_e^2 = 0.75\Xi_d^2[1.31 + 1.61\Xi_u/\Xi_d + 1.01(\Xi_u/\Xi_d)^2]\,. \qquad (4.1)$$

where Ξ_u and Ξ_d are the deformation-potential constants as defined by Herring.[18] The effective mass is taken to be the density-of-states effective mass.

The results of Herring and Vogt are not directly extendable to the case being treated here since we are dealing with a Fermi degenerate distribution of electrons and the temperatures are low enough that equipartition is not valid for the phonons of

interest. However, numerical estimates of the terms in Eq. (3.8) for the electrons show that this model provides a good estimate (i.e., within a factor of 2) at 2 °K. At lower temperatures the differences between transverse and longitudinal sound velocities are sufficiently large that this model can lead to substantial errors.

B. Model for holes

For the hole contribution, we use an approximation originally introduced by Lawaetz[22] and Wiley.[23,27] The valence band is approximated by one spherical heavy-hole band with the spherically averaged effective mass. The light-hole band can be neglected since it has very few holes in it. The velocity of sound is taken to be the average longitudinal sound velocity. The deformation potential is taken to be an average value appropriate to the calculation of the hole mobility[23]

$$\Xi_h^2 = 0.29[a^2 + 2.6(b^2 + \tfrac{1}{2}d^2)] \ , \tag{4.2}$$

where a, b, and d are the deformation-potential constants defined by Pikus and Bir.[21]

C. Screening

The potential due to the screening charge must be estimated for the models given above. In the formal expression, Eqs. (2.11) and (2.12), $c_\lambda(\vec{q})$ will depend in general on the details of the anisotropy, deformation potentials, and matrix elements in Eq. (2.7) and (2.8). The value of $c_\lambda(\vec{q})$ is sensitive to the relative sign of the electron and hole contributions. Hence, to estimate the role of screening using our model parameters, we must make a judicious choice of the sign of the parameters. To make this determination, we compare the relative phases of the diagonal matrix elements of deformation potential for holes with the deformation potential for electrons.

For electrons in the [111] valley[19]

$$D^e = (\Xi_d + \tfrac{1}{3}\Xi_u)(\epsilon_{xx} + \epsilon_{yy} + \epsilon_{zz}) + \tfrac{1}{3}\Xi_u(\epsilon_{xy} + \epsilon_{yz} + \epsilon_{xz}) \ , \tag{4.3}$$

where the strain tensors are referred to crystallographic axis along the [100] directions. The matrix elements for other valleys can be obtained from a symmetry transformation and the dilational parts are invariants. For the heavy-hole band[20,21]

$$D^h(\vec{k},\vec{k}) = \left(a + \frac{Bb(3\hat{k}_x^2 - 1)}{2[B^2 + C^2(\hat{k}_x^2\hat{k}_y^2 + \text{c.p.})]^{1/2}}\right)\epsilon_{xx} + \frac{Dd\hat{k}_x\hat{k}_y}{[B^2 + C^2(\hat{k}_x^2\hat{k}_y^2 + \text{c.p.})]^{1/2}}\epsilon_{xy} + \text{c.p.} \ , \tag{4.4}$$

where c.p. stands for cyclic permutations of x, y, and z; B, C, and D are effective-mass parameters for hole bands[20]; $\hat{k}_x$ are unit vectors.

For longitudinal modes, since the dilational part dominates and both $\Xi_d + \frac{1}{3}\Xi_u$ and a in Eqs. (4.3) and (4.4) are negative in Ge (see Table I for parameters), we may regard the deformation-potential constants for electrons and holes as having the same sign. For the transverse modes, the relative signs of D^e and D^h are determined by the shear components. They depend on the direction of $\vec{k}$ of the valence bands and on the valleys of the conduction band. We know from symmetry that the transverse phonons along [100], [110], and [111] directions are not screened, as shown in Sec. II. We also know, for example, that the [111] transverse phonons do not scatter electrons in the [111] valley from symmetry, and have little effect for other valleys. However, for most of the phonons propagating in arbitary directions, the transverse phonon cannot be exactly defined, and it is not obvious that the screening is vanishing small in general. For simplicity, we adopt the approximation that half of the transverse scattering has D^e and D^h

TABLE I. List of parameters used in calculation.

ϵ_F^e	ϵ_F^h	n	m_e	m_h	U
2.5 meV [a]	3.9 meV [a]	2.4×10^{17} cm^{-3} [a]	$0.22m$ [b]	$0.30m$ [b]	5×10^5 cm/sec [c]
ρ	κ	Ξ_d	Ξ_u	a	b	d
5.3 g/cm^3 [d]	15.36 [e]	−8.5 eV [f]	19 eV [f]	−2.0 eV [g]	2.2 eV [g]	4.4 eV [g]

[a] Reference 26.
[b] M. Combescot and P. Nozières, J. Phys. C. 5, 2369 (1972).
[c] Reference 19.
[d] S. M. Sze, *The Physics and Semiconductor Devices* (Wiley, New York, 1969), p. 57.
[e] W. F. Brinkman and T. M. Rice, Phys. Rev. B 7, 1508 (1973).
[f] Reference 24.
[g] Reference 23.

to be of the same sign and half has the opposite sign. Assuming that each mode contributes the same weight in scattering, the signs of Ξ_e and Ξ_h are determined as follows: two-thirds of the total scattering events are assumed to have Ξ_e and Ξ_h of the same sign, and one-third is of the opposite sign. What is important is that Ξ_e and Ξ_h have the same sign for most of the scattering. This corresponds to the bands' edges moving in opposite directions as a result of the phonon perturbations.

This approximation probably overestimates the effect of screening since we are allowing the transverse phonons to be screened in part. However, as will be shown by the results later, the screening effect is small even in this approximation (reducing the damping by less than a factor of 2). Therefore, the errors caused by our approximation for screening of transverse mode is less than a factor of 2. Other approximations in our model may introduce errors of comparable size.

The matrix element defined in Eq. (2.4) may be computed using the two band approximations introduced by Kane.[28] In this approximation we consider only the single heavy-hole band and $O_{\vec{k}+\vec{q}n,\vec{k}n'}$ in Eq. (2.4) turns out to be independent of $\vec{k}$. The result may be written as:

$$O(q)=\tfrac{1}{2}(1+3\cos^2\gamma)^{1/2}, \tag{4.5}$$

where γ is the angle between $\vec{k}$ and $\vec{k}+\vec{q}$ on the Fermi surface. This addition is found to make a small correction to our final results.

Hence, finally we have for the screened carrier-phonon interaction in Eqs. (2.15) and (2.16)

$$M^e(\vec{k}+\vec{q},\vec{k})=(\hbar/2\rho\omega)^{1/2}q[\Xi_e+V_+(q)] \tag{4.6}$$

and

$$M^h(\vec{k}+\vec{q},\vec{k})=(\hbar/2\rho\omega)^{1/2}q[\Xi_h-V_+(q)O(q)], \tag{4.7}$$

where $V_\pm(q)$ are calculated by Eq. (2.11) and represent potentials arising for polarization of EHD; the plus and minus subscripts in $V_\pm$ denote the two values of $V(q)$ obtained by assuming that Ξ_e and Ξ_h are of the same sign and of opposite sign from the values discussed above. The density of the crystal is given by ρ.

D. Calculation for the damping coefficient

Using the matrix elements in Eqs. (4.6) and (4.7), one can carry out integrations in Eq. (3.8) for the damping rate γ in our model. The damping coefficient obtained is of the same form as Keldysh's formula[11,12]

$$\gamma=\frac{1}{12\pi^3}\,\frac{q_{\rm th}^5}{\hbar^2(m_e+m_h)\rho U n}(\nu m_e^2\Xi_e^2K_e+m_h^2\Xi_h^2K_h), \tag{4.8}$$

where

$$q_{\rm th}=kT/\hbar U. \tag{4.9}$$

In the formula, m_e and m_h are the mass for electrons and holes defined in our model; ν is the number of equivalent valleys ($\nu=4$ in Ge); the T, ρ, and U are the temperature, density, and longitudinal sound velocity of the crystal; n is the carrier pair density in EHD. The K_e and K_h are integrals reduced from Eq. (3.8). They are calculated by assuming that two-thirds of the scattering events use V_+ and one-third use V_- as described in Sec. IV C.

$$K_h=\frac{2}{3}\int_0^{\zeta_h}\frac{\zeta^5[1-V_+(\zeta)O(\zeta)/|\Xi_h|]^2}{(e^\zeta-1)(1-e^{-\zeta})}d\zeta + \frac{1}{3}\int_0^{\zeta_h}\frac{\zeta^5[1-V_-(\zeta)O(\zeta)/|\Xi_h|]^2}{(e^\zeta-1)(1-e^{-\zeta})}d\zeta, \tag{4.10}$$

where

$$\zeta_h=2k_{Fh}/q_{\rm th} \tag{4.11}$$

and k_{Fh} is the Fermi wave vector for holes. The overlap integral $O(\zeta)$ can be obtained from Eq. (4.5)

$$O(\zeta)=\tfrac{1}{2}\{1+3[1-2(\zeta/\zeta_h)^2]\}^{1/2}. \tag{4.12}$$

The two functions $V_+(\zeta)$ and $V_-(\zeta)$ are given by

$$V_+(\zeta)=\frac{8\pi e^2n}{\kappa q_{\rm th}^2\epsilon(\zeta)\zeta^2}\left(\frac{|\Xi_h|}{W_h(\zeta)}-\frac{|\Xi_e|}{W_e(\zeta)}\right), \tag{4.13}$$

$$V_-(\zeta)=\frac{8\pi e^2n}{\kappa q_{\rm th}^2\epsilon(\zeta)\zeta^2}\left(\frac{|\Xi_h|}{W_h(\zeta)}+\frac{|\Xi_e|}{W_e(\zeta)}\right). \tag{4.14}$$

The $W_h(\zeta)$, $W_e(\zeta)$ result from the two summations in Eq. (2.12). For spherical band structure, they are given by

$$\frac{1}{W_e(\zeta)}=\frac{3}{4E_{Fe}}\left(\tfrac{1}{2}+\frac{\zeta_e^2-\zeta^2}{4\zeta_e\zeta}\ln\left|\frac{\zeta_e+\zeta}{\zeta_e-\zeta}\right|\right) \tag{4.15}$$

and

$$\frac{1}{W_h(\zeta)}=\frac{3}{4E_{Fh}}\left(\frac{1}{2}+\frac{\zeta_h^2-\zeta^2}{4\zeta_h\zeta}\ln\left|\frac{\zeta_h+\zeta}{\zeta_h-\zeta}\right|\right), \tag{4.16}$$

where E_{Fe} and E_{Fh} are the Fermi energies for electrons and holes, respectively. Neglecting the small overlap integral effect, the dielectric function in Eq. (2.12) can be reduced to

$$\epsilon(\zeta)=1+\frac{8\pi e^2n}{\kappa q_{\rm th}^2}\left(\frac{1}{W_e(\zeta)}+\frac{1}{W_h(\zeta)}\right). \tag{4.17}$$

The same equations hold for K_e; the function $O(q)$ in Eq. (4.10) is absent and the appropriate electron parameters are substituted.

V. DAMPING OF HIGH-VELOCITY DROPLETS

When the drift velocity is larger than the sound velocity and comparable to the EHD Fermi vel-

ocity, the previous linear calculation is not valid. To treat the damping in this case, we calculate the momentum loss rate due to phonon scattering. The distribution functions for electrons and holes are taken to be drifted Fermi distribution functions both shifted to produce the same average velocity. The carrier-carrier scattering is assumed to maintain a distribution function which is simply a drifted Fermi distribution and to keep the electrons and holes moving at the same velocity. The momentum loss rate for the holes and electrons will be computed independently and simply added together.

Since screening of the carrier-phonon interaction in Ge will modify the result of calculation by only a factor of 2 or less, and other approximations introduce uncertainties of comparable size, we will use the much simpler "bare" interaction in the high-velocity calculation. The same model for band structure of Ge in Sec. IV is used here. The square of matrix elements of $V_{e\text{-ph}}$ in Eq. (2.7) for an electron scattered from $\vec{k}$ to $\vec{k}+\vec{q}$ by phonon absorption averaged over themal phonon occupation probability may be written as

$$|\langle N_{\vec{q}}-1;\vec{k}+\vec{q}|V_{e\text{-ph}}|\vec{k};N_{\vec{q}}\rangle|^2=\frac{\Xi_e^2\hbar q}{2\rho U}\ \frac{1}{e^{\hbar Uq/kT}-1} \tag{5.1}$$

where Ξ_e is given by Eq. (4.1), ρ, and are U the density and longitudinal sound velocity of the crystal, and the volume of the crystal is assumed to be unity. Similarly for phonon emission, we have

$$|\langle N_{\vec{q}}+1;\vec{k}+\vec{q}|V_{e\text{-ph}}|\vec{k};N_{\vec{q}}\rangle|^2=\frac{\Xi_e^2\hbar q}{2\rho U}\left(\frac{1}{e^{\hbar Uq/kT}-1}+1\right). \tag{5.2}$$

The rate of momentum loss by the electrons in the EHD in one conduction valley can be written down using the usual result of time-dependent perturbation theory[29]:

$$\frac{d\vec{P}_e}{dt}=\frac{2\pi}{\hbar}\sum_{\vec{k},\vec{q}}\hbar\vec{q}\,[\,|\langle N_{\vec{q}}-1;\vec{k}+\vec{q}|V_{e\text{-ph}}|\vec{k};N_{\vec{q}}\rangle|^2\delta(E(\vec{k})-E(\vec{k}+\vec{q})+\hbar Uq)+|\langle N_{\vec{q}}+1;\vec{k}+\vec{q}|V_{e\text{-ph}}|\vec{k};N_{\vec{q}}\rangle|^2$$
$$\times\delta(E(\vec{k})-E(\vec{k}+\vec{q})-\hbar Uq)]f(\vec{k})[1-f(\vec{k}+\vec{q})]\,, \tag{5.3}$$

where $f(\vec{k})$ is the shifted Fermi distribution function. The shift is taken to be $m_e v/\hbar$ and v is the drift velocity of the drops. Similar equations can be written down for holes with the hole parameters replacing the electron parameters.

The rate of momentum loss by the carriers in the EHD is balanced by the damping of the EHD velocity.

$$\frac{dP_e}{dt}+\frac{dP_h}{dt}=(m_e+m_h)n\Omega\,\frac{dv}{dt}\,, \tag{5.4}$$

where Ω denotes the volume of the droplet. To determine the damping of the EHD, we must compute the rate of momentum loss by the carriers from Eq. (5.3). The rate of momentum loss by the carriers is a nonlinear function of v.

The integrations involved in the evaluation of the rate of momentum loss in Eq. (5.3) are complicated for arbitrary values of the drift velocity limits. In the low-velocity case, this approach gives linear damping with the same value obtained in Sec. IV.

In the high-velocity limit, the shift of the Fermi function is larger than the thermal broadening, and we can simplify the calculation by neglecting the thermal broadening of the shifted carrier distribution function. In addition, we neglect the phonon energy compared with electronic energies; this is a reasonable approximation when the drift velocity is considerably larger than sound velocity. The details of our estimate of the integrals are given in the Appendix. We only give the results here.

The rate of momentum loss for electrons is given by

$$\frac{d\vec{P}_e}{dt}=-C_e[F_1(S)+F_2(S)]\hat{v}\,, \tag{5.5}$$

where the dimensional constant C_e is given by

$$C_e=16\nu k_{Fe}^6\Xi_e^2 m_e\Omega/(2\pi)^3\hbar\rho U \tag{5.6}$$

and ν is the number of equivalent valleys (4 in Ge). The unit vector $\hat{v}$ is in the direction of the drift velocity. The parameter S is defined to be

$$S=v/v_{Fe}, \tag{5.7}$$

where v_{Fe} is the Fermi velocity for electrons. The functions F_1 and F_2 are defined in the Appendix.

The same expressions hold for the momentum loss rate for holes in droplets, except that parameters for holes are used. The integrals in Eq. (5.5) and the analogous equation for the hole contribution may be carried out numerically to give the rate of momentum loss in Eq. (5.4).

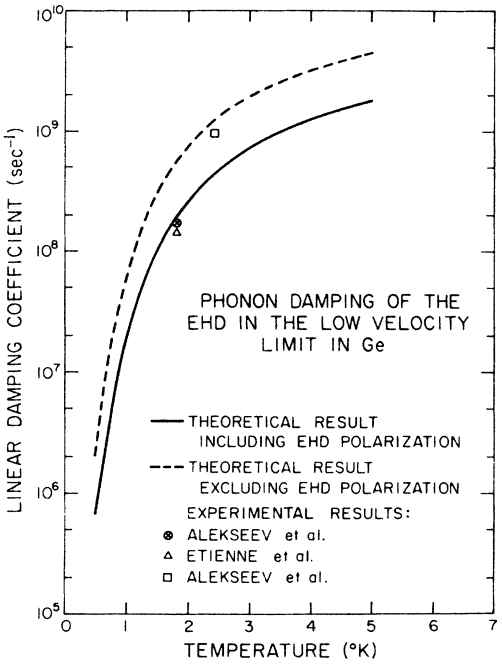

FIG. 1. Phonon damping coefficient for EHD motion in Ge vs temperature in the low-drift-velocity limit. The dashed curve is the result for the "bare" carrier-phonon interaction; the solid curve is the result when screening of the carrier-phonon interaction by the carriers in the EHD is included. The experimental points are ⊗ from Ref. 2, △ from Ref. 4, and □ from Ref. 5.

VI. RESULTS AND DISCUSSION

A. Low velocity

The values of parameters used in the calculation are given in Table I. The one-dimensional integrals in the expressions for K_e and K_h were calculated numerically. The result of the calculation of the damping coefficient in pure Ge, as a function of temperature, is plotted in Fig. 1. For comparison, the result of damping coefficient without including screening is also indicated by dashed line. Experimental results by Alekseev *et al.*[2,3] using 160-MHz ultrasonic absorption, by Alekseev *et al.*[5] using droplet motion in a nonuniform stressed crystal, and by Etienne *et al.*[4] using 1.5-GHz ultrasonic absorption are shown in Fig. 1 for comparison.

First of all, we see that screening of carrier-phonon interaction in the EHD has reduced the damping by only about a factor of 2. The screening effect is rather small in Ge, because the valence and conduction bands tend to move in opposite directions when Ge is subjected to an arbitrary deformation. Thus, the two types of carriers tend to move in the same direction in response to a deformation and the net induced charge is small.

Second, we see that the results of calculation are in reasonable agreement with the values of the damping rate determined by ultrasonic absorption experiments and droplet motion in an inhomogeneous deformation. In our model, we used the averaged deformation-potential constants in Eqs. (4.1) and (4.2). The averaging involved in them is slightly different from the "averaging" prescribed in Eq. (3.8). This approximation is still reasonable for temperatures around and above 2°K. In the low-temperature limit (below 1°K), one may expect the transverse modes of phonons will dominate because the smaller value of transverse sound velocity (about 3.5×10^5 cm/sec in Ge).

The calculated damping coefficient is approximately three orders of magnitude larger than that obtained if the junction noise experiments[8] and Doppler-shifted light scattering experiments[9] are interpreted in terms damped motion without a driving force. Hence, we conclude the droplet motion in those experiments were pushed by an external force, most likely the force from the interaction of a stream of nonequilibrium phonon—the phonon wind.[6] This effect has been investigated recently. In the junction noise experiments, since pulsed (10 nsec) excitation is used, it is most likely that the phonon wind produced in nonradiative recombination of electrons and holes in the nonuniform distribution of EHD pushes the droplets a distance of about 0.3 mm. A rough estimate using Keldysh phonon wind theory[6] gives results in qualitative agreement with the experimental observations. Worlock *et al.*[30] has estimated the role of phonon wind in the Doppler-shifted light scattering experiments and finds qualitative agreement with the experimental observations.

Very recently Hensel and Dynes[31] have measured the interaction of phonons with EHD. Using an estimate of the phonon wind, they conclude that the damping at 1.6°K is approximately 8.3×10^8 sec^{-1}. This value is in qualitative agreement with the results presented here.

B. High velocity

Evaluating the results stated in Sec. V for the parameters in Table I, we obtain the results shown in Fig. 2. Since we find that spontaneous emission dominates the damping, we expect the results to be almost independent of temperature. Hence, while the results in Fig. 2 are obtained for 0°K, they are in fact valid for the temperature range where EHD occur, $T \lesssim 7$°K. At zero

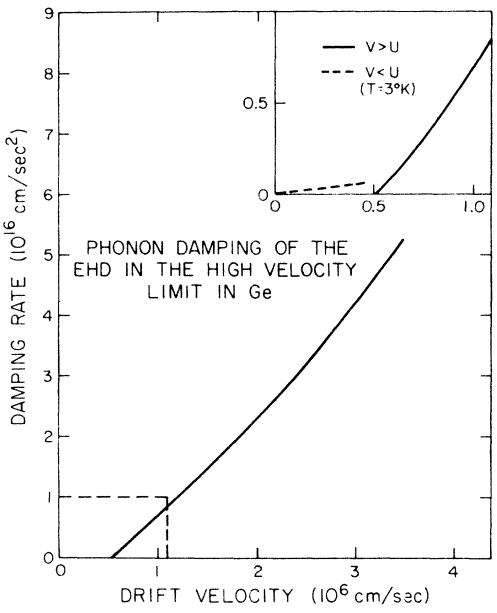

FIG. 2. Damping rate for EHD motion in Ge vs drift velocity in the high-velocity limit ($V_d > U$). The calculation was carried out for zero temperature, but the damping rate is insensitive to temperature when $V_d \gg U$. There is no phonon damping of the EHD motion at zero degrees when $V_d < U$. The insert compares the low-velocity damping rate at $T = 3$ °K curve with that at high drift velocities.

degrees, there is no damping of EHD motion for $v_d < U$. For comparison, we show the low-velocity result for $T = 3$ °K in the insert of Fig. 2.

The main point of this figure is that the damping rate increases very rapidly when the droplet velocity exceeds the sound velocity. This sudden increase is due to the large number of phonon emission processes which become kinematically possible when v is greater than U. If a droplet were moving at velocities greater than the sound velocity, its motion should be very rapidly damped.

Comparing with the experiment,[10] we find the effective damping observed in Ref. (10) is smaller than our theoretical phonon damping by at least two orders of magnitude. Therefore, the experimental results cannot be explained without assuming an external force, most likely from phonon wind.[6]

Based on our results, we believe that the initial drift velocities, larger than the sound velocity, reported in Ref. 10 should be reinterpreted. They are obtained by fitting the data and extrapolating to the initial time of droplet motion. The phonon wind cannot push the droplet to a velocity exceeding the sound velocity in the crystal. Even if some other forces, for instance, the pressure from a highly degenerate electron-hole plasma, impart the droplet with an initial velocity exceeding the sound velocity, the droplet should quickly relax to sound velocity in about 0.1 nsec for the damping obtained here. Therefore, the extrapolation to obtain the initial velocity in Ref. 10 is not valid.

Further, the subsequent motion of the drops described in Ref. 10 may be explained by the force provided by the phonon wind generated from the nonradiative recombinations of carriers inside the other droplets which were distributed nonuniformly. The phonon wind generated during the thermalization of excited nonequilibrium carriers should not have a significant role in determining the subsequent motion of drops, because the phonon wind produced by this process lasts only about 0.3 μsec and drop motion is observed for a period of several microseconds. To give a rough estimate of this phonon wind effect, we can make use of the results of Bagaev *et al.*[6] In that experiment[6] they find that the phonon wind can push the drops to a distance of about 1 mm with phonons produced by a continuous laser with power of about 40 mW. In the experiment in Ref. 10, the drops are pushed to a distance of about 2 mm when the carrier was generated by a YAG:Nd laser with a pump power of 20 W. The total number of carriers generated by this pump pulse is about 3×10^{13}. The recombination lifetime of drops in Ge is about 40 μsec, a significant contribution of which is due to nonradiative process.[32] The phonon generated from the nonradiative recombination of all drops created by the pump pulse of 20 W is estimated to be between 40 and 80 mW. Since the powers going to phonon generation are about the same in the two experiments, we would expect the distances the EHD would be pushed would be comparable. This observation is in agreement with the experimental results.

C. Summary

We have calculated the phonon damping in the low- and high-velocity limit. We find that the theoretical value of the damping in the low velocity agrees with that observed in ultrasonic absorption and stress induced droplet motion experiments. We find that the screening changes the damping by about a factor of 2.

For high velocities, our calculations show that damping is very rapid if the droplet goes faster than sound velocity. Spontaneous phonon emission dominates the damping. The damping is sufficiently large that we think it unlikely droplet velocities greater than the sound velocity will be observed.

VII. ACKNOWLEDGMENTS

The authors gratefully acknowledge useful discussions with J. M. Worlock. This work was supported in part by the Office of Naval Research. One of us (T. C. McGill) wishes to acknowledge the support of the Alfred P. Sloan Foundation.

APPENDIX: EVALUATION OF INTEGRALS FOR THE MOMENTUM LOSS RATE

In this Appendix, we evaluate the rate of momentum loss by electrons in the EHD given by Eq. (5.3) in the high-velocity case. Similar results hold for the momentum loss rate by the holes.

It is convenient to divide the sums in Eq. (5.3) into two terms and to rewrite Eq. (5.3) as

$$\frac{dP_e}{dt} = I_1 + I_2 . \tag{A1}$$

Here I_1 includes all the phonon absorption and stimulated phonon emission process. Since the square of stimulated phonon emission matrix element equals that of phonon absorption, I_1 is given by

$$I_1 = \frac{2\pi}{\hbar} \sum_{\vec{k},\vec{q}} (\hbar\vec{q})(|\langle N_{\vec{q}} - 1; \vec{k}+\vec{q}|V_{e-ph}|\vec{k}; N_{\vec{q}}\rangle|)^2 [\delta(E(\vec{k}) - E(\vec{k}+\vec{q}) + \hbar Uq) + \delta(E(\vec{k}) - E(\vec{k}+\vec{q}) - \hbar Uq)] f(\vec{k})[1 - f(\vec{k}+\vec{q})] . \tag{A2}$$

The term I_2 includes all the "spontaneous" phonon emission process. The square of matrix elements for these processes is the difference of the values in Eq. (5.1) and Eq. (5.2). We can write I_2 as

$$I_2 = \frac{2\pi}{\hbar} \sum_{\vec{k},\vec{q}} (\hbar\vec{q}) \left(\frac{\Xi_e^2 \hbar q}{2\rho U} \right) \delta(E(\vec{k}) - E(\vec{k}+\vec{q}) - \hbar Uq) \times f(\vec{k})[1 - f(\vec{k}+\vec{q})] , \tag{A3}$$

where the parameters are defined in Eq. (6.2). In the high-velocity limit, I_2 makes a larger contribution to the momentum relaxation than I_1. However, we will estimate I_1 before I_2 because some of the results for I_1 can be used in evaluating I_2.

The sum of the terms in I_1 which contain the product $f(\vec{k})f(\vec{k}+\vec{q})$ is identically zero. In the high-velocity limit, the small thermal spreading of the electron distribution function is unimportant, and we replace this distribution function with its zero-temperature value. The integral I_1 then becomes

$$I_1 \simeq \frac{2\pi}{\hbar} \sum_{\vec{k},\vec{q}} (\hbar\vec{q}) \{ |\langle N_{\vec{q}} - 1; \vec{k}+\vec{q}|V_{e-ph}|\vec{k}; N_{\vec{q}}\rangle|^2 [\delta(E(\vec{k}) - E(\vec{k}+\vec{q}) - \hbar Uq) + \delta(E(\vec{k}) - E(\vec{k}+\vec{q}) + \hbar Uq)] \theta(k_{Fe} - |\vec{k} - m_e\vec{v}/\hbar|) \} , \tag{A4}$$

where the θ function is the Heavyside function defined in the usual way: $\theta(x) = 0$ for $x < 0$; $\theta(x) = 1$ for $x \geq 0$.

This integral in Eq. (A4) can be carried out straightforwardly. Applying the standard approximation of neglecting phonon energy,[33] the result is simply

$$I_1 = -C_e F_1(S)\hat{v} , \tag{A5}$$

where the dimensional constant C_e is given in Eq. (5.6) and the dimensionless integral $F_1(S)$ is given by

$$F_1(S) = \int_{1-S}^{1+S} R_e(y) A(y,S)\, dy . \tag{A6}$$

Here the variable y is the wave vector of electrons measured in units of Fermi wave vector k_{Fe}, i.e., $y = k/k_{Fe}$; S is defined in Eq. (5.7). The function $A(y,S)$ is given by

$$A(y,S) = 1 - [(y^2 + S^2 - 1)/2yS]^2 . \tag{A7}$$

The function $R_e(y)$ is an integral given by

$$R_e(y) = \frac{1}{(\zeta_e)^5} \int_0^{y\zeta_e} \frac{Z^4}{e^Z - 1}\, dZ , \tag{A8}$$

where ζ_e is defined in Eq. (4.11).

The summation of the $f(\vec{k})f(\vec{k}+\vec{q})$ product terms do not vanish for I_2. In the high-velocity limit, we can neglect the small temperature spreading of the electron distribution function in I_2, and also neglect the phonon energies. The sum of the $f(\vec{k})f(\vec{k}+\vec{q})$ product terms vanishes in this ap-

proximation, and the integral I_2 can be put into the same form as in Eq. (A4)

$$I_2 = \frac{2\pi}{\hbar} \sum_{\vec{k},\vec{q}} (\hbar\vec{q}) \left(\frac{\Xi_e^2 \hbar q}{2\rho U} \right) \delta(E(\vec{k}) - E(\vec{k}+\vec{q})) \times \theta\left(k_{Fe} - |\vec{k} - m_e \vec{v}/\hbar| \right) . \quad \text{(A9)}$$

The result of the integration of Eq. (A9) is

$$I_2 = -C_e E(S) \hat{v} , \quad \text{(A10)}$$

where the integral $E(S)$ is given by

$$E(S) = \int_{1-S}^{1+S} Q_e(y) A(y, S)\, dy . \quad \text{(A11)}$$

The function $Q_e(y)$ is given by

$$Q_e(y) = \tfrac{1}{10} y^5 . \quad \text{(A12)}$$

The above results are valid for drift velocities considerably larger than the sound velocity. For the case when the drift velocity nearly equals the sound velocity, the approximation of neglecting the finite phonon energy for I_1 is still valid. The limits of integration on two contributions (phonon absorption and spontaneous phonon emission) to I_1 are such that the first-order terms in the ratio of sound velocity to Fermi velocity vanish. However, for I_2, this approximation is not valid. For the spontaneous phonon emission process, the effect of finite phonon energy is important when the droplet velocities are comparable with the sound velocity.

We can obtain a qualitative interpolation of the results for I_2 between the low- and high-velocity limit. The dominant contribution for the momentum loss rate comes from carrier scatterings from the direction of the drift velocity to the opposite of that direction. For a Fermi sphere shifted by S, $S = v/v_{Fe}$ as defined in Eq. (5.7), those carriers in the states with $\vec{k}$ in the direction of the velocity $\hat{v}$ can scatter into a vacant state in the opposite direction. Carriers undergoing this scattering must have a momentum larger than a minimum value Z (measured in the units of Fermi momentum), where Z is determined by the energy conservation equation

$$(\hbar^2 k_{Fe}^2/2m_e)(1-S)^2 + 2\hbar U k_{Fe} = (\hbar^2 k_{Fe}^2/2m_e) Z^2 . \quad \text{(A13)}$$

To express Z in terms of S, we have

$$Z = [(1-S)^2 + 4U/v_{Fe}]^{1/2} . \quad \text{(A14)}$$

Therefore, the carriers with momentum less than $\hbar Z k_F$ should not make a significant contribution to the momentum loss rate. Because of the finite phonon energy, it is a much better approximation to exclude that contribution than to include it with the neglect of phonon energy. An improved approximation for Eq. (A11) is therefore to replace $E(S)$ by $F_2(S)$ such that

$$F_2(S) = \int_Z^{1+S} Q_e(y) A(y, S)\, dy . \quad \text{(A15)}$$

This replacement of the lower limit of integration from $1 - S$ to Z provides a reasonable interpolation between the results from the calculations of the low- and high-velocity limit.

[1]See, for example, Ya. Pokrovskii, Phys. Status Solidi A 11, 385 (1972); and V. S. Bagaev, Springer Tracts Mod. Phys. 73, 72 (1975).

[2]A. S. Alekseev, T. I. Galkina, V. M. Maslennikov, R. G. Khakomov, and E. E. Shchebev, Pis'ma Zh. Eksp. Teor. Fiz. 21, 578 (1975)[JETP Lett. 21, 271 (1975)].

[3]A. S. Alekseev, T. I. Galkina, Fiz. Tverd, Tela. (Leningrad) 18, 2005 (1976) [Sov. Phys.-Solid State 18, 1167 (1976)].

[4]B. Etienne, L. M. Sander, C. Benoit a la Guillaume, M. Voos, and J. Y. Prisur, Phys. Rev. Lett. 37, 1299 (1976).

[5]A. S. Alekseev, V. S. Bagaev, and T. I. Galkina, Zh. Eksp. Teor. Fiz. 63, 1020 (1972) [Sov. Phys.-JETP 36, 536 (1973)].

[6]V. S. Bagaev, L. V. Keldysh, N. N. Sibel 'din, and V. A. Tsvetkov, Zh. Eksp. Teor. Fiz. 70, 702 (1976) [Sov. Phys.-JETP 43, 362 (1976)].

[7]V. B. Fuks, Pis'ma Zh. Eksp. Teor. Fiz. 20, 33 (1974) [JETP Lett. 20, 14 (1974)].

[8]J. M. Hvam, and I. Balslev, Phys. Rev. B 11, 5053 (1975).

[9]J. Doehler, J. C. V. Mattos, and J. M. Worlock, Phys. Rev. Lett. 38, 726 (1977).

[10]T. C. Damen, and J. M. Worlock, in the *Proceedings of the Third International Conference on Light Scattering in Solids*, edited by M. Balkanski, R. C. Leute, and S. P. Porto (Flammarion, Paris, 1976), pp. 183-188.

[11]L. V. Keldysh, and S. G. Tikhodeev, Pis'ma Zh. Eksp. Teor. Fiz. 21, 582 (1975) [Sov. Phys.-JETP Lett. 21, 273 (1975)].

[12]L. V. Keldysh, in *Excitons in Semiconductors*, (Nauka, Moscow, 1974), pp. 5–19.

[13]J. Bardeen, Phys. Rev. 52, 688 (1937).

[14]See, for example, J. M. Ziman, *Electrons and Phonons* (Oxford University, London, 1963).

[15]In principle κ would depend on q, but for our purpose here, since we will be dealing with small q, we can neglect this variation.

[16]See, for example, D. Pines and P. Nozières, *The Theory of Quantum Liquids I* (Benjamin, New York,

1966).
[17]See, for example, M. Lax, *Symmetry Principles in Solid State and Molecular Physics*, (Wiley, New York, 1974). This statement is not true for zinc-blende structures along the [110].
[18]C. Herring, Bell Syst. Tech. J. 34, 237 (1955).
[19]C. Herring and E. Vogt, Phys. Rev. 101, 944 (1956).
[20]G. L. Bir and G. E. Pikus, Fiz. Tverd. Tela 2, 2287 (1960) [Sov. Phys.-Solid State 2, 2039 (1961)]. A similar theory was worked out independently by M. Tiersten, IBM J. Res. Dev. 5, 122 (1961).
[21]G. E. Pikus and G. L. Bir, Fiz. Tverd. Tela 1, 1642 (1959) [Sov. Phys.-Solid State 1, 1502 (1960)].
[22]P. Lawaetz, Phys. Rev. 174, 867 (1968).
[23]J. D. Wiley, Solid State Commun. 8, 1865 (1970).
[24]M. Costato, S. Fontanesi, and L. Reggiam, J. Phys. Chem. Solids 34, 547 (1973).
[25]G. Dresselhaus, A. F. Kip, and C. Kittel, Phys. Rev. 98, 368 (1955).
[26]G. A. Thomas, T. G. Phillips, T. M. Rice, and J. C. Hensel, Phys. Rev. Lett. 31, 386 (1973).
[27]J. D. Wiley, Phys. Rev. 4, 2485 (1971).
[28]E. O. Kane, J. Phys. Chem. Solids 1, 249 (1957).
[29]See, for example, L. I. Shiff, *Quantum Mechanics* (McGraw-Hill, New York, 1949).
[30]J. M. Worlock, J. Doehler, and J. C. V. Mattos, Bull. Am. Phys. Soc. 22, 349 (1977).
[31]J. C. Hensel and R. C. Dynes, Phys. Rev. Lett. 39, 969 (1977).
[32]C. Benoit à la Guillaume, M. Voos, and F. Salvan, Phys. Rev. Lett. 27, 1214 (1971).
[33]See, for example, E. M. Conwell in *Solid State Physics* (Academic, New York, 1967), Suppl. Vol. 9, Chap. III.